Received: 20 November 2019 | Revised: 28 December 2019 | Accepted: 24 January 2020

DOI: 10.1111/jace.17044

ORIGINAL ARTICLE

Journal of the American Ceramic Society

Aligning α-alumina platelets via uniaxial pressing of ceramic-filled polymer blends for improved sintered transparency

William J. Costakis Jr. | **Andrew Schlup** | **Jeffrey P. Youngblood** | **Rodney W. Trice**

School of Materials Engineering, Purdue University, West Lafayette, IN, USA

Correspondence
William J. Costakis Jr., School of Materials Engineering, Purdue University, West Lafayette, IN, USA.
Email: wcostaki@purdue.edu

Funding information
Army Research Office, Grant/Award Number: W911NF-17-0205

Abstract

Uniaxial warm pressing was used to align alumina platelet-filled polyethylene-based copolymer blends. The solids loading (30-40 vol.%) and platelet diameter (1.2 and 11 μm) were varied to compare effects on viscosity, percent reduction, and final alignment. All ceramic-filled thermoplastic polymer blends exhibited pseudoplastic behavior. Crystallographic alignment of green body samples was quantified by the orientation parameter (r) and grain misalignment angle (full width at half maximum, FWHM) obtained from rocking curve analysis. Blends with 11 μm diameter platelets displayed a higher temperature sensitivity constant, better flow properties, and higher alignment compared to blends with 1.2 μm diameter platelets. Optimal samples produced with blends containing 30 vol.% of 11 μm diameter platelets demonstrated an alignment of $r = .251 \pm .017$; FWHM = 11.16° ± 1.16°. A sample with optimal alignment was hot-pressed to transparency and obtained an in-line transmission of 70.0% at 645 nm. The final alignment of this pre-aligned hot-pressed sample ($r = .254 \pm .008$; FWHM = 11.38° ± 0.54°) improved when compared to a non-pre-aligned sample ($r = .283 \pm .005$; FWHM = 13.40° ± 0.38°).

KEYWORDS

optical materials/properties, rheology/rheometry, alumina, hot pressing

1 | INTRODUCTION

As discussed in our previous work,[1] transparent alumina is an ideal material for ballistic protection applications where visible or infrared wavelength transmission is required.[2–4] However, to achieve these favorable properties, alumina must be sintered to high densities (>99.99%TD) to eliminate light scattering due to porosity.[5] Even at high densities, the transparency of alumina is limited due the rhombohedral crystal structure being inherently birefringent.[6] Birefringence causes light scattering at misaligned grain boundaries due to differences in refractive index and is detrimental to the transparency of polycrystalline alumina.[2,6–8] Fundamental equations developed by Apetz and Van Bruggen[8] related the transparency of alumina to the refractive index difference and grain size. It has been shown experimentally that the crystallographic alignment of equiaxed alumina powders with a high magnetic field prior to densification reduces birefringent light scattering.[6,7,9] However, this method may be limited in terms of scalability. Ultimately, there is a need to develop a forming method that will allow for large-scale and cost-effective production of transparent alumina with high crystallographic alignment.

In our previous work,[1] we discussed the effects of hot-pressing parameters on the densification behavior and optical performance of platelet morphology alumina. This work was performed with the hypothesis that alternative processing methods that use shear or elongational stresses could be used to pre-align these platelet alumina powders. Textured or oriented ceramics have increasingly gained interest due to the enhanced properties they offer in magnetic, structural,

piezoelectric, and optical materials.[7,10–14] Due to the demand for highly oriented ceramics, several methods have been used to develop textured ceramics. Initial investigations on techniques such as hot working (compression or tensile)[15–17] led to the development of general texture in electronic and structural materials. Shear forming techniques using anisotropically shaped particles have resulted in highly textured electronic and composite materials.[18–21] One of the most commonly used methods to fabricate highly textured technical ceramics is templated grain growth (TGG).[10–12,22–24] Typically, this process disperses 1-15 vol.% (of the total solids content) of morphologically anisotropic powders (seeding particles) in an equiaxed submicrometer powder matrix.[10–12,22–24] Shear forming techniques, such as dry forming,[22] screen printing,[10] and slip or tape casting,[10,23–25] are used to physically align the anisotropic powders within the matrix. During the pressureless sintering process, the anisotropic single crystal powders grow and develop a high-volume fraction of crystallographic texture. This process, when paired with tape casting, is able to obtain highly textured (FWHM $\leq 10°$) alumina samples.[10,26,27] However, TGG is not a feasible processing method for transparent alumina due to the liquid phase formers (typically aluminosilicates) required to promote anisotropic grain growth and preserve particle anisotropy.[10–12,22,24] The addition of these sintering aids causes the formation of secondary phases that result in degradation of the optical transmission.[8]

We propose using a forming process that utilizes shear and elongational stresses to align platelet alumina such that after subsequent hot-pressing, a dense, highly textured sample with improved optical properties is obtained.[1] Tape casting is one of the most frequently used and successful shear forming processes for obtaining microstructural and crystallographic texture.[18–21,23,28–35] This process could be a possible candidate for the development of texture in transparent alumina. However, a bulk of the literature focuses on seeding an equiaxed matrix with a small amount of aligned anisotropic powders. Unfortunately, few articles report on the fabrication of tape cast samples consisting of entirely platelet morphology powders.[18,29,35]

Watanabe et al[18] successfully tape cast slurries with solids loading ranging from 15 to 33 vol.% $BiTiO_3$ (4 μm diameter) platelets. This study performed a combination of XRD and SEM texture analysis to characterize their green body and sintered samples. They obtained a maximum orientation degree (f) of roughly 0.9.[18] The methods that were used to characterize these samples are considered semiquantitative at best and have been known to inflate the data when $f \geq 0.9$.[12,26,27] Therefore, it is difficult to compare this data to values of strong texture and to assess the extent of texture. Other studies performed by Fu and Roosen[29] on tape casting of alumina produced green body samples of 20 vol.% platelets (8.7 μm). However, they did not report the quantitative alignment of the samples since the primary focus was on binder burnout defects. A more recent study by Wonisch et al[35] tape cast 28 vol.% alumina platelets (2.2 μm) to compare experimental and simulated data. They used image analysis software on optical micrographs of cross-sections to determine an orientation angle with respect to the casting direction. Their results showed that anisotropic particles showed a higher degree of particle orientation when compared to equiaxed. However, the highest value reported was roughly 32°, with 0° being the maximum aligned state in the casting direction.[35] Even though this study was able to obtain a relatively high solids loading for the tape casting process, the orientation values that they calculated were low when compared to other shear forming processes.[10,12,22] At the current moment, it is not clear if tape casting is capable of processing highly aligned samples from entirely platelet alumina powders while maintaining a suitable solids loading (>30 vol.%).

However, ceramic-filled thermoplastic polymer blends have been used by the fibrous monolith and coextrusion community for some time.[13,14,36–44] Many of these processes have taken advantage of the shear and elongational stresses developed during forming to align anisotropic powders. One study by Trice and Halloran[14] used a simple process termed warm pressing to develop qualitative alignment in systems consisting of a 50 vol.% hexagonal boron nitride and polymer additives mixture. They found that warm pressing the ceramic-filled polymer blends before hot-pressing led to a qualitative increase in the grain alignment, which contributed to an increase in crack deflection during flexure testing.[14] This warm pressing technique was also used to fabricate silicon carbide and oriented boron nitride multilayered composites to investigate crack deflection and propagation mechanisms.[45] In both of these studies, they did not quantitatively characterize the alignment of the sample but argued that other studies showed highly textured samples through similar processes.[46] Other studies on the coextrusion of silicon nitride and boron nitride fibrous monoliths claimed that the shear stresses developed during the coextrusion process lead to the alignment of anisotropically shaped boron nitride and β-silicon nitride powders.[46] However, the alignment developed in these studies is also not fully understood as only a simple qualitative XRD texture analysis was performed instead of a pole figure analysis due to limitations associated with boron nitride basal plane intensities. Regardless, it is apparent that the shear and elongational stresses produced during processing influence the alignment of the final microstructure, yet investigation on the texture development is needed to determine if methods such as warm pressing or coextrusion can obtain highly aligned microstructures.

What is apparent from the literature on ceramic-filled thermoplastic processing is that warm pressing may be ideal for the axisymmetric alignment of platelet alumina powders for improved transparency. This simple process uses heated platens to apply a compressive load to a ceramic-filled thermoplastic blend. Upon compression, the blend flows and elongates in

the non-constrained directions. It is expected that this flow behavior will induce elongational stresses via biaxial extensional flow[47,48] as well as shear stresses via capillary flow.[18,49,50] These flow stresses should lead to velocity gradients that can preferentially align high aspect ratio platelets parallel to the direction of flow according to Jeffery's analysis on orientation dynamics.[50,51] Pre-aligned alumina brown bodies produced via warm pressing of a well-developed rheological blend will yield increased particle alignment and hence increase the in-line transmission when compared to previous studies on hot-pressed platelet alumina.[1] We believe this method will be a strong candidate for producing large sheets of textured alumina over magnetic alignment methods.[6,7,9]

The present study aims to produce axisymmetric-aligned platelet alumina in ceramic-filled thermoplastic polymer sheets via uniaxial warm pressing. The blends were modified from compositions of poly(ethylene-co-ethyl acrylate) (EEA) found in the literature.[36,44] This was done via plasticizer additions and acrylate reductions, resulting in desirable flow properties and greater formability. The developed blends have a platelet alumina loading ranging from 30 to 40 vol.% and a constant amount of polymer additives, with a balance of base polymer (EEA). This study assesses the effects of alumina platelet diameter and solids loading on the rheological properties, percent reduction in thickness, and final platelet orientation of ceramic-filled polymer sheets produced via warm pressing. Finally, a sample with the best pre-alignment conditions was hot-pressed to transparency and compared to a non-pre-aligned sample hot-pressed under the same conditions.

2 | EXPERIMENTAL PROCEDURE

2.1 | Mixing of ceramic-filled polymer blends

The platelet powders used in this study were RonaFlair White Sapphire alumina (Merck KGaA) with a manufacturer-reported purity of 99.8% and grade YFA02050 Serath alumina (Kinsei Matec Co., Ltd) with a manufacturer-reported purity of 98.0%. Both powders have a platelet morphology, as seen in Figure 1. The RonaFlair or large platelet powder has a reported diameter of 11 μm and a thickness of approximately 0.5 μm while the Serath or small platelet powder has a reported diameter of 1.2 μm and a thickness of approximately 0.07 μm. BET surface areas of 2.00 ± 0.02 m^2/g and 11.47 ± 0.05 m^2/g were obtained for RonaFlair and Serath powders, respectively, using a TriStar II 3020 gas adsorption analyzer (Micromeritics Instrument Corporation). To have a comparison between platelet and equiaxed powders, AA-03 (Sumitomo Chemical Co., Ltd.) alumina was used. This powder has a manufacturer-reported purity of 99.99%, diameter of 0.44 μm, and BET surface area of 5.2 m^2/g.

A thermoplastic binder system was modified and adapted from previous work on the coextrusion of fibrous monoliths[13,14,37–42,52,53] and green machining.[43] The development of the system and individual functions of each component is described in detail in the literature.[36,44] A four-component polymer blend consisting of EEA (MFI = 6.0 g/10 min, poly[ethylene-co-ethyl acrylate], Dow Elastomers, Midland, MI), PiBMA (poly[ethylene-co-butyl acrylate], Acryloid B67, Rohm and Haas), poly ethylene glycol (PEG1300, Mw = 1300 g/mol, Sigma-Aldrich), and HMO (heavy mineral oil, Fischer Chemical, Hampton, NH) was selected. Typically, a wax-based component (stearic acid) is added to act as a lubricant during shear mixing; however, this component was removed due to negative effects associated with polymer stability during mixing, pressing, and binder removal.

A Brabender high-shear torque rheometer (Plasti-Corder PL 2100 Electronic Torque Rheometer, C. W. Brabender) was used to initially mix the ceramic-filled polymer blend. A detailed schematic of this setup with geometrical data is presented in other literature.[42] During mixing, the shear mixer was equipped with a banbury blade geometry. Initial mixing parameters of 130°C and 20 RPM were selected. The total amount of EEA was added and allowed to thoroughly blend. Once mixed, small increments of the selected powders were continuously added to the system. Throughout the entire mixing process, PiBMA and PEG1300 were slowly introduced. After all the powder was added to the system, the roller speed was increased to 60 RPM and the remaining HMO was added. The blend was mixed at these parameters until the torque value stabilized

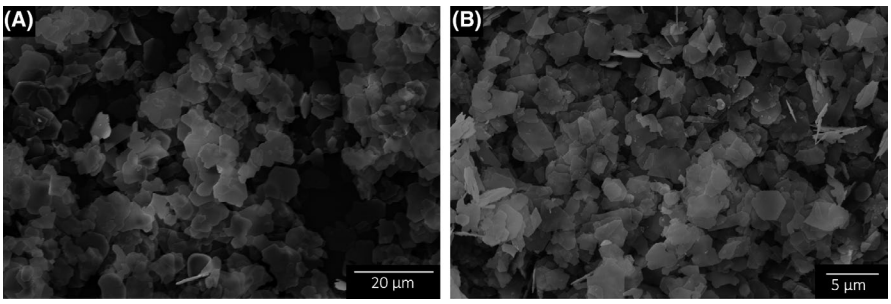

FIGURE 1 SEM micrographs of (A) RonaFlair (large) alumina platelets with a reported average particle diameter of 11 μm and (B) Serath (small) alumina platelets with a reported average particle diameter of 1.2 μm

(approximately 15 minutes). It was then removed from the mixer and chopped into roughly 1 cm^2 pieces for further processing. The compositions of the ceramic-filled polymer blends are listed in Table 1.

2.2 | Torque viscometry of ceramic-filled polymer blends

The viscosity-shear rate dependence of the mixed blends was measured using the torque rheometer. Examples in the literature[42,54–59] have shown that mixers equipped with a torque meter and relatively small chamber are viable tools when used to obtain the viscosity-shear rate behavior from the torque-RPM data in polymer-based systems. However, Xu and Hilmas[42] and Santi et al[59] showed that this type of analysis is not entirely accurate when large amounts of ceramic powder are introduced to the system but is still a feasible method to use as a comparative analysis between similar systems.

For the analysis, the torque rheometer was equipped with a roller-type mixing head with the same dimensions shown in the literature.[42] The sample chamber was loaded to 70% of the total volume (60 cm^3) with the ceramic-filled polymer blend and mixed at an initial temperature of 130°C with a roller speed of 20 rpms for 20 minutes. Once the torque and temperature were stable, the rotor speed was decreased to 10 rpm and mixed for an additional 5 minutes. Torque data were collected at 120°C, 130°C, 140°C, and 155°C for 10 minutes to characterize the torque-temperature dependence. An exponential fit of the torque vs temperature graph was used to obtain the viscosity temperature sensitivity constant (b). This constant was used to account for temperature increases due to viscous dissipation and to correct the measured viscosity in future measurements through the following equation:

$$\Gamma(T) = \Gamma(T)\exp\left[-b\left(T - T_o\right)\right] \tag{1}$$

where $\Gamma(T)$ is torque as a function of temperature, b is the viscosity temperature sensitivity constant, T is the set temperature, and T_o is the measured temperature of the blend.[59] After the torque-tperature analysis, the temperature was set to 130°C and the roller speed was decreased to 5 RPM. Torque data were collected at 5, 10, 20, 30, 50, and 70 RPM in 5 minute intervals to obtain the torque-RPM dependence of each blend. To obtain the shear-rate and viscosity data, the analysis suggested by Bousmina et al[56] was applied. In their analysis, they introduce a universal quantity that they termed the effective equivalent internal radius or R_i. This internal radius is useful because it is insensitive to the rheological behavior of the blend and is only dependent on the geometrical dimensions and gear ratio of the torque rheometer.[42,56,59] Calculating R_i is essentially a means of calibrating the torque rheometer. In the current study, a Newtonian silicone oil was used to obtain R_i from the following equation:

$$R_i = \frac{R_c}{\left[1 + \frac{4\pi N}{n}\left(2\pi \cdot mLR_c^2 \cdot \frac{1+g^{n+1}}{\Gamma}\right)\right]^{\frac{n}{2}}}, \tag{2}$$

where R_c is the chamber radius, N is the roller speed per second, n is the power law index, m is the melt consistency index, L is the roller length, Γ is the torque exerted on the roller shaft, and g is the gear ratio.[42,56,59] Once R_i was obtained, it was used in the following equations to calculate the shear rate (Equation 3) and viscosity (Equation 4) for each ceramic-filled polymer blend.

$$\dot{\gamma} \approx \frac{2\pi N}{\ln\left(\frac{R_c}{R_i}\right)}, \tag{3}$$

$$\eta = \frac{\Gamma}{N}\frac{\left(\frac{R_c}{R_i}\right)^2 - 1}{8\pi^2 LR_c^2 \cdot \left(1 + g^2\right)}. \tag{4}$$

A linear fit of the log(viscosity) dependence on the log(shear rate) was used to obtain the power law index (n) and melt consistency index (m) for each blend.

TABLE 1 Ceramic-filled thermoplastic blend compositions and measured viscosity data

Powder type	Al_2O_3 [vol.%]	EEA [vol.%]	PiBMA [vol.%]	HMO [vol.%]	PEG [vol.%]	b [$°C^{-1}$]	R^2	n	log(m)	R^2
RonaFlair 11 μm (large)	40	44.9	4.6	0.5	10.0	0.012	.991	0.38	3.981	.995
	35	49.9	4.6	0.5	10.0	0.012	.976	0.46	3.806	.996
	30	54.9	4.6	0.5	10.0	0.015	.963	0.56	3.539	.997
Serath 1.2 μm (small)	40	44.9	4.6	0.5	10.0	0.006	.921	0.14	4.745	.999
	30	54.9	4.6	0.5	10.0	0.008	.998	0.38	4.357	.980
AA03 0.44 μm (equiaxed)	40	44.9	4.6	0.5	10.0	0.016	.999	0.65	3.867	.997

Notes: The viscosity data were collected on a torque rheometer, where b is the viscosity temperature sensitivity constant, n is the power law index, and m is the flow consistency index.

2.3 | Uniaxial warm pressing of ceramic-filled polymer blends

A modified version of the process referred to as warm pressing[13,14,45] was used to align the platelet alumina. The blend was placed in a 7.6 × 3.8 cm stainless steel die and held in a continuous load (250 kg) at 150°C for 1 hour to form a preform. The preform, roughly 17.9 mm thick, was removed from the die and placed between two metal plates coated with polytetrafluoroethylene (PTFE). Universal mold release (Smooth-On, Inc) was added to the surface of the PTFE to aid with lubrication and sample removal. For all blend compositions, a hydraulic press was used to apply a load of 4500 kg to the assembly at 150°C and held for approximately 15 minutes to form a sheet. Each sheet was shimmed to (2.0, 1.5, or 1.0 mm) obtain a homogenous thickness. Due to the PTFE layers, the expected target thicknesses were roughly 1.4, 0.9, and 0.4 mm. The ability for a blend to reach the target thickness was dependent on the rheology of the system and the final thickness was reported in percent overall reduction. The ceramic-filled polymer sheets were cooled under load to room temperature at which point, the load was removed and the sheets were separated from the metal plates.

2.4 | Texture distribution analysis

A texture analysis was performed to gain an understanding of the effect of processing conditions on the alignment. A rocking curve analysis was conducted on the (000.12) plane using a Panalytical Empyrean Diffractometer (Malvern Panalytical Ltd). The machine was equipped with a bent Ge incident beam monochromator that is tuned to transmit Cu$K\alpha_1$ radiation. For both scans, incident slit geometry was fixed to 0.5° or 0.75 mm while the detector active length was set to 0.715 mm. A high-resolution 2θ scan was collected at the Bragg's peak of interest (2θ = 90.6°, the basal plane that is perpendicular to the orientation plane). The data collection range was ± 1.24° with a step size of 0.005° and a dwell time of 1.0 second. This scan was used to accurately locate the (000.12) plane and the 2θ axis was locked on the center of this peak for the following omega scan. The omega scan or rocking curve tilt range was ± 43.13°, with a step size of 0.25° and a dwell time of 1.0 s. Preliminary analysis showed no repeatable treads in regard to alignment and sample position. Therefore, 10 separate rocking curve analyses were performed on the 10 green body samples collected from random locations on the pressed sheets to obtain an average value for the different processing conditions. For sintered samples, three separate rocking curve analyses were performed on both sides of the samples in different locations.

The data were corrected for defocusing and absorption phenomena in TexturePlus,[60] a software package developed at the National Institute of Standards and Technology, through explicitly determining the intensity distribution of the high-resolution 2θ scan (Bragg's peak).[27] Following this correction, the obtained texture profiles were fit to the March-Dollase equation displayed below:

$$F(f,r,\omega)=f\left(r^2\cos^2\omega+\frac{\sin^2\omega}{r}\right)^{-\frac{3}{2}}+(1-f), \qquad (5)$$

where f is the volume fraction of textured grains ($f = 1$), r is the orientation parameter, and ω is the specimen tilt angle or the angle between the texture axis and x-ray scattering vector.[12,26,61] The orientation parameter is obtained from the curve fit and is used to access the alignment of the samples. An average orientation parameter was obtained from the 10 green body samples and was used to characterize each sheet. For sintered samples, an average orientation parameter (r) was obtained from the six total scans from both sides of the samples. It is important to note that a lower orientation parameter corresponds to a higher alignment (r = 0; prefect alignment, r = 1; random orientation).[12,26,61]

2.5 | Binder burnout and hot-pressing

Multiple 2.5 cm diameter disks were punched from the ceramic-filled polymer sheets and individual disks were stacked on a crucible. The polymer was removed by heating at a rate of 1.5°C/h to 500°C in flowing air, followed by an isothermal hold for 1 hour. To mimic the procedure by Schlup et al,[1] 6 g of the brown body disks was heat treated at 1100°C for 1 hour in air prior to being placed in the graphite hot-press die. The exact details of the die assembly and hot-pressing process can be found elsewhere.[1] Samples were hot-pressed with a preload pressure of 0 MPa, a maximum temperature of 1800°C, an isothermal hold time of 7 hours, and a maximum pressure of 10 MPa. A vacuum atmosphere was maintained from room temperature to 1550°C, then backfilled with flowing nitrogen for the remainder of the hot-press run. For comparison, loose RonaFlair powder was poured into a graphite die and hot-pressed under the same parameters described above.

2.6 | Optical analysis

Hot-pressed samples, as well as a sapphire standard, were ground and polished to a 1 μm diamond suspension ultimate surface polish. Optical measurements over the visible spectrum (200-800 nm) were performed with a PerkinElmer Lambda 950 UV-VIS-NIR spectrophotometer equipped with an integrating sphere. Total transmission, in-line transmission, reflection, and absorption were measured and from this, forward and backward scattering values were derived. All optical values are normalized to a thickness of 0.8 mm

and reported at a wavelength of 645 nm, similar to the literature.[8,62,63] The exact details of this analysis are given in the previous publication.[1]

3 | RESULTS AND DISCUSSION

To take advantage of shear and elongational stresses, it is desirable to have blends that exhibit thermoplastic polymer-like properties or behave more like the base polymer (EEA). Blends made with greater than 40 vol.% platelet powders (both RonaFlair and Serath blends) produced samples with processing defects and were considered unworkable. Many of these samples would crumble during removal from the warm pressing surfaces. However, samples made with equiaxed (AA03) powders were able to reach higher solids loading and maintain polymer-like properties, which is similar to what is observed in the literature for EEA-based systems.[14,36,39,41,42,44–46] The use of platelet morphology powders is clearly influencing the behavior of the blends. As will be shown in a later section, blends, where the polymer characteristics dominate, resulted in higher alignment. Therefore, it is important to quantify the rheological behavior and connect it to the processing parameters and particle alignment.

3.1 | Viscosity dependence on temperature

The torque-temperature dependence for RonaFlair (large) and Serath (small) blends is shown in Figure 2 at different solids loading. These curves reveal that each blend experiences a decrease in torque as temperature increases at a constant roller speed. This behavior is common for thermoplastic polymers and can be related to the weak intermolecular forces between polymer chains.[42,56,64] The solid lines correspond to an exponential fit of the data with all curve fits having an R^2 value > 0.92. The measured viscosity temperature sensitivity constant (b) for each blend is shown in Table 1. These values were used to determine the extent of the polymer-like properties of each blend and to correct the torque vs roller speed data to a reference temperature of 130°C by Equation 1.

Table 1 shows that an increase in solids loading decreases the temperature sensitivity constant for both platelet types. A higher b corresponds to higher viscous dissipation, which is typically explained by the thermal motion of polymer chains, chain flexibility, and the degree of chain entanglement.[59,65] Therefore, in ceramic-filled blends with higher b, polymer interactions will dominate. To keep the total batch volume constant, a decrease in platelet solids loading was balanced with an increase in EEA. Adding more polymer to the system should increase the amount of polymer chain interactions, allowing polymer interactions to dominate over the mechanical interactions of the ceramic powders.[42] It is also possible

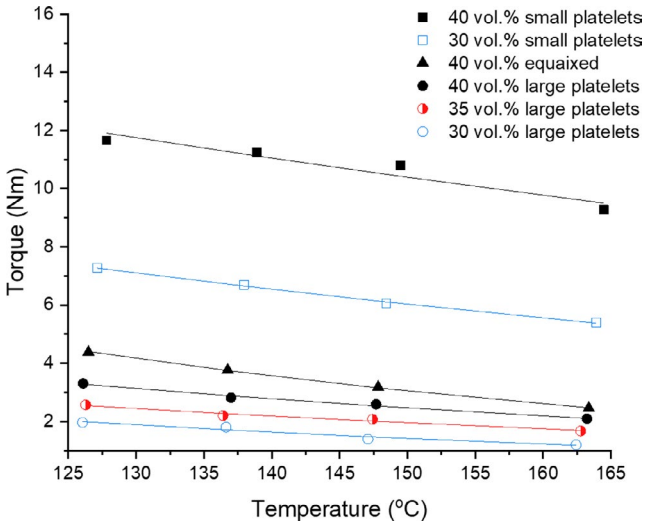

FIGURE 2 Torque vs temperature dependence of large platelets, small platelets, and equiaxed blends at different solids loading measured on a Brabender torque rheometer at a constant rotor speed of 10 RPM. These curves reveal that each blend experiences a decrease in torque as temperature increases. The viscosity temperature sensitivity constant (b) for each blend is shown in Table 1

that increasing powder content leads to an increase in particle-particle and particle-polymer interactions. These interactions could lead to a decrease in polymer entanglement which will result in less viscous dissipation.

In Table 1, blends made with large platelets have a higher b than blends made with small platelets, regardless of solids loading. As stated above, polymer interactions will be more dominant in ceramic-filled blends with higher b. Blends made with large platelets have fewer individual particles than blends made with small platelets (at a constant vol.%) due to the difference in particle size. Fewer particles could lead to the polymer interactions dominating over the particle-particle interactions in large platelet blends. Likewise, an increase in the total amount of particles in small platelet blends leads to more particle-polymer interactions and decreases chain entanglement.[42,65] These mechanisms may explain why b and the viscous dissipation are greater for large platelet blends, and smaller for small platelet blends. However, this behavior is not observed in the equiaxed blend, which has the highest b (0.016°C^{-1}) of all blends and lowest particle size (0.44 μm). This behavior must be a characteristic feature of platelet morphology powders. As stated earlier, it is desirable to have blends where the polymer interactions dominate. Therefore, blends with the highest b (large platelet) were considered ideal for forming processes to achieve particle alignment.

Figure 2 shows that an increase in the solids loading led to an increase in the measured torque for the different platelet blends. This trend is commonly observed in similar ceramic-filled polymer blends developed for coextrusion[39,42,55] and green machining processes.[36] A study focusing on the rheological

behavior of $BaTiO_3$/EEA blends found that an increase in solids loading increased the torque and viscosity values at a constant temperature.[42] They claimed this behavior was due to an increase in the mechanical interparticle interactions between the ceramic powders. In the literature, it is typical to have solids loading greater than 50 vol.% in EEA-based blends and still have workable samples,[14,36,39,41,42,44–46] which is not the case for the blends produced in the current study. Blends produced with greater than 40 vol.% platelets had measured torque values lower than or equal to observed torque values for 55 vol.% equiaxed powder blends from the literature,[42] and were still considered unworkable. Clearly, the use of platelets vs equiaxed powders is influencing the behavior of the blends.

3.2 | Rheological measurements

Figure 3 shows the log(viscosity) dependence on log(shear rate) at 130°C for large and small platelet blends at different solids loading. A 40 vol.% equiaxed blend is added for comparison. The solid lines correspond to linear curve fits with all $R^2 > 0.98$. The powder law index (or shear thinning exponent, n) and melt consistency index (m) were calculated from the fits and are shown in Table 1. All ceramic-filled polymer blends exhibited a pseudoplastic or shear thinning behavior with $n < 1$. It is important to note that the shear thinning exponent obtained by a torque rheometer has been found to not be in agreement with the data obtained on a parallel plate rheometer, as described by Xu and Hilmas.[42] They claimed that this deviation from the expected behavior is probably due to the blends having

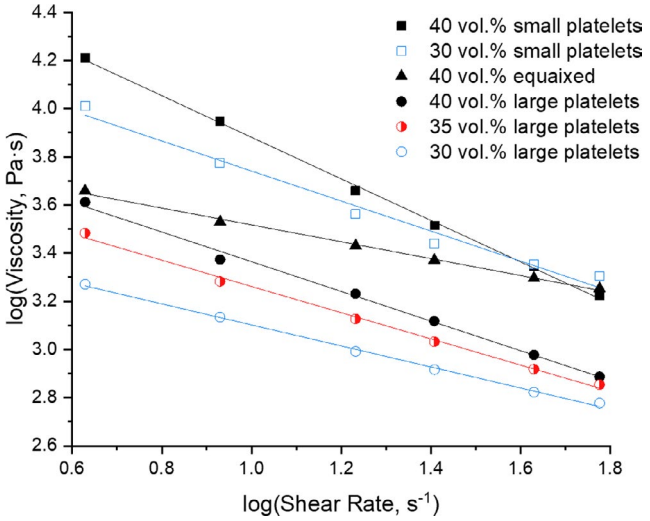

FIGURE 3 Log(viscosity)-log(shear rate) dependence of large platelets, small platelets, and equiaxed blends at different solids loading measured on a Brabender torque rheometer at 130°C. Increasing the solids loading resulted in an increase in viscosity for respective platelet type. All polymer blends exhibited a uniform shear thinning behavior with $n < 1$

yield stresses, as well as the relationship between log(torque) and log(shear rate) being non-linear at lower shear rates.[42] However, they did find that the melt consistency indexes and the overall trends obtained by a torque rheometer and parallel plate rheometer were in agreement.

From Figure 3 it was found that an increase in solids loading led to an increase in the viscosity for a given shear rate, regardless of powder type. This behavior is commonly observed in the literature for ceramic-filled polymer blends and could be attributed to the increased polymer-particle interactions, interparticle interactions, and collisions.[42] It was also found that an increase in solids loading led to a decrease in the shear thinning exponent (n) and an increase in the flow consistency index (m) for both platelet powders, as shown in Table 1. Both trends are observed in the literature for blends that were developed for coextrusion.[39,42,55]

Blends made from large platelets exhibited lower viscosity values than blends made with small powders, regardless of solids loading and shear rate. Recall in Section 3.1, blends made with large platelets will have fewer individual particles due to the difference in particle size. Fewer particles could lead to fewer particle-particle interactions. Additionally, it is known that geometrical characteristics of ceramic powders have a significant effect on particle packing density, particle arrangement, and rheological properties.[19] Anisometric particles with the ability to freely rotate will readily orient due to imparted shear stresses.[50,51] Since the large platelet blends experience less particle-particle interactions, the platelets should be able to rotate more freely and eventually orient parallel to the direction of shear. Xu and Hilmas[42] claimed that particle orientation can result in laminar flow and lead to a reduction in the resistance to shear. It is possible that the large platelet blends have lower viscosities because there are fewer particles and the morphology of the particles is more susceptible to orientation.

Figure 3 shows that the 40 vol.% equiaxed blend has a higher viscosity than the large platelet blends and a lower viscosity than the small platelet blends. According to previous logic on particle size and particles per volume, the equiaxed powder should have a higher viscosity than both platelet blends, which is not the case. This is most likely due to the difference in particle morphology, specifically, the surface area. Recall in Section 2.1, the surface area of the equiaxed powders being higher than the large platelets and lower than the small platelets. These differences in surface area could explain the viscosity behavior. It is well understood in the field of colloidal processing that increasing the specific surface area leads to increases in the number of particle-particle interactions and thus increases the viscosity.[66,67] Additionally, the flow behavior of the equiaxed blends is different than the platelet blends. The 40 vol.% equiaxed blend had the highest shear thinning exponent ($n = 0.65$) and the lowest flow consistency index ($\log(m) = 3.867$) of all blends, as shown in Table 1. It is well understood that anisotropic

powders will be susceptible to shear stresses and align, decreasing the resistance to shear, resulting in significantly more shear thinning when compared to spherical powders.[42,66] Even though the equiaxed blend has a higher viscosity than all the large platelet blends and experiences less shear thinning than all blends, it was the most workable blend. This behavior could be due to the equiaxed blend experiencing more viscous dissipation and dominating polymer interactions. It may be possible to use mixtures of equiaxed and platelet powders to develop blends with more optimized rheological properties or behaviors similar to the base polymer (EEA) in future studies.

As stated above, blends made with platelet solids loading greater than 40 vol.% were considered unworkable. They also may have experienced issues with polymer degradation. This behavior was most apparent in blends produced with 40 vol.% small platelets. At higher shear rates, the viscosity values are lower for the 40 vol.% small platelet blends than the 30 vol.% small platelet and 40 vol.% equiaxed blends. This behavior was not expected. During the analysis, the roller speed, which is proportional to the shear rate, is slowly increased from low to high RPM over the course of 180 minutes. Visual inspection showed that the behavior of the 40 vol.% small platelet blend changed from the beginning of the analysis to the end. After the rheological test, this blend had a chalk-like appearance and behaved more as a dry powder blend (crumbled apart) than a polymer blend. The shear thinning exponent ($n = 0.14$) was the lowest in this study and lower than blends produced in the literature,[39,42,55] indicating that this blend is more prone to degradation than the other blends in this study.

3.3 | Texture analysis of pressed sheets

The orientation parameter (r) and grain misalignment angle (full width at half maximum [FWHM]) were obtained from a rocking curve analysis and these values are listed in Table 2. A lower orientation parameter (r) and lower FWHM are associated with higher alignment. For this analysis, the alignment reference plane was normal to the pressing direction. As mentioned earlier, 10 samples were analyzed from each pressed sheet to obtain an average r and FWHM. Each blend (solids loading and platelet type) was pressed to a target thickness of roughly 1.4, 0.9, and 0.4 mm (accounting for the PTFE coating) to obtain a percent reduction of 92.2, 95.0, and 97.8%, respectively. The final pressed sample thickness was measured and is reported in Table 2 as percent reduction.

Figure 4 shows the average orientation parameter vs percent reduction for large platelet blends made with different solids loading. For all large platelet solids loadings (30, 35, 40 vol.%), each blend was able to reach the target reduction of 92.2% (within ~0.5%); however, this is not true for other target reductions. An example of this is shown in Table 2 where both the 40 and 35 vol.% blends were not able to reach a target reduction of 97.8%. Instead, these samples reached a final reduction of 94.8 and 95.4%, respectively. For these samples, the metal plates did not fully seat on the shims under the applied load (4000 kg). It was evident that these blends required a higher load to reach larger reductions. However, preliminary tests showed that forcing the sample to flow at higher loads may be negatively impacting the alignment, which could be due to particle jamming.[68] Additionally, blends with 30 vol.% large platelets were able to reach all the

TABLE 2 Texture distribution data for ceramic-filled thermoplastic blends uniaxially pressed to varied thicknesses

Powder type	Shim (mm)	vol.%	Reduction (%)	FWHM (°)	r	R^2
RonaFlair 11 μm (large)	1.4	40	92.40 ± 0.05	23.28 ± 1.20	.401 ± .013	>.99
		35	92.62 ± 0.03	19.53 ± 1.01	.360 ± .012	>.99
		30	92.77 ± 0.04	14.32 ± 0.52	.295 ± .007	>.98
	0.9	40	94.16 ± 0.08	21.59 ± 1.40	.383 ± .015	>.98
		35	95.09 ± 0.04	19.80 ± 0.94	.363 ± .011	>.99
		30	95.25 ± 0.03	15.34 ± 0.48	.309 ± .006	>.99
	0.4	40	94.79 ± 0.13	21.80 ± 1.43	.384 ± .015	>.99
		35	95.41 ± 0.52	19.26 ± 1.43	.356 ± .018	>.98
		30	97.01 ± 0.10	11.16 ± 1.16	.251 ± .017	>.99
Serath 1.2 μm (small)	1.4	40	91.30 ± 0.08	25.39 ± 0.89	.420 ± .009	>.98
		30	92.47 ± 0.03	20.24 ± 1.06	.368 ± .012	>.98
	0.4	40	91.72 ± 0.32	25.99 ± 1.35	.429 ± .013	>.98
		30	95.09 ± 0.28	20.99 ± 0.98	.379 ± .006	>.98
AA03 0.44 μm (equiaxed)	0.4	40	97.04 ± 0.20	– ± –	– ± –	–

Notes: Orientation parameter (r) obtained from curve fits of the March-Dollase equation. The 95% confidence interval of the reduction, FWHM, and orientation parameter are shown for each sample having a data population of 10.

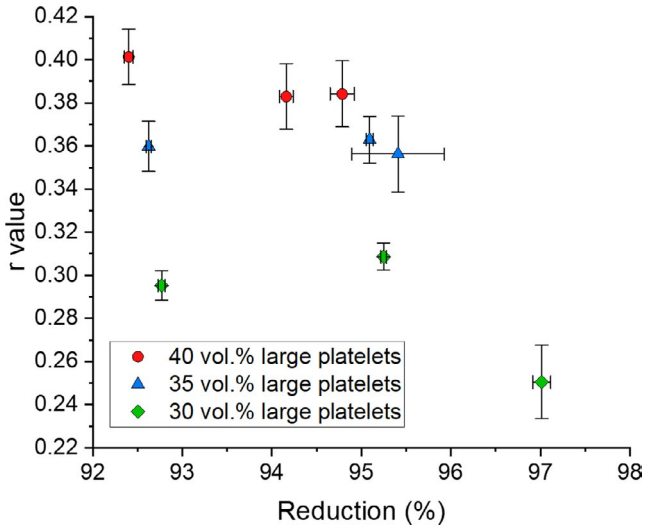

FIGURE 4 Orientation parameter (r) vs percent reduction dependence of large platelet blends at different solids loading. The 95% confidence interval for both the orientation parameter and percent reduction is shown for each sample having a data population of 10

target percent reductions under the applied load. It seems that the ability of each blend to reach the target percent reduction is connected to the extent of the polymer behavior (temperature sensitivity constant [b]) and flow properties (shear thinning exponent (n) and flow consistency index [m]), which is related to the solids loading (ie, polymer content) and leads to differences in the final alignment. To support this claim, the 40 vol.% equiaxed blend was pressed to a target reduction of 97.7% and was able to reach an average reduction of 97.04% (reported in Table 2). This value is similar to the percent reduction obtained from the 30 vol.% large platelet blend when pressed to the same target percent reduction. Both of these blends had higher temperature sensitivity constants and shear thinning exponents.

It was found that decreasing the solids loading resulted in sheets that were able to undergo more reduction and obtain lower orientation parameters. As mentioned above, decreasing the ceramic solids loading led to an increase in the temperature sensitivity constant (b) and increased the flow properties (higher shear thinning exponents (n) and lower flow consistency indexes (m)), which resulted in pressed sheets with higher percent reductions. Decreasing the ceramics solids loading may have allowed the polymer interactions to dominate, resulting in blends that reach higher reductions and undergo more biaxial extensional flow during warm pressing. It is expected that this increased amount of flow allows for higher velocity gradients that will induce alignment of platelets.[50,51] It is also possible that decreasing solids loading decreases particle-particle interactions,[42] allowing the platelets to rotate more freely and align parallel to the direction of flow.[50,51]

Also observed in Figure 4 is that the pressed sheets tend to reach a characteristic minimum orientation parameter for different solids loadings. Further increases in the reduction do not result in further alignment, which is apparent in the 40 and 35 vol.% large platelet blends. Sheets produced with 40 and 35 vol.% solids loading had a characteristic minimum orientation parameter of roughly 0.39 and 0.36, respectively. It seems that this minimum alignment was obtained at a target reduction of 92.2%, and further alignment was not obtained with an increase in percent reduction. However, sheets produced with 30 vol.% solids loading did experience further alignment after pressing to target percent reductions higher than 95.0%. It appears that the 30 vol.% blend experiences a characteristic minimum orientation parameter at higher percent reductions, (>97%). As suggested above, decreasing the solids loading will lead to a decrease in the particle-particle interactions, allowing the platelets to rotate and further align. This could explain why the lower solids loading blends are able to reach a higher alignment.

Figure 5 shows the average orientation parameter vs percent reduction for sheets developed from small and large platelet blends. From the plot, it is clear that blends developed with small platelets experience far less alignment when compared to the large platelet blends with the same solids loading. For small platelet blends, the same trends with solids loading, temperature sensitivity constant, flow properties, and target percent reduction that were observed in large platelet blends are present. However, blends produced with small platelets experience inferior rheological properties when compared to large platelet blends. All small platelet blends had lower temperature sensitivity constants and poorer flow properties

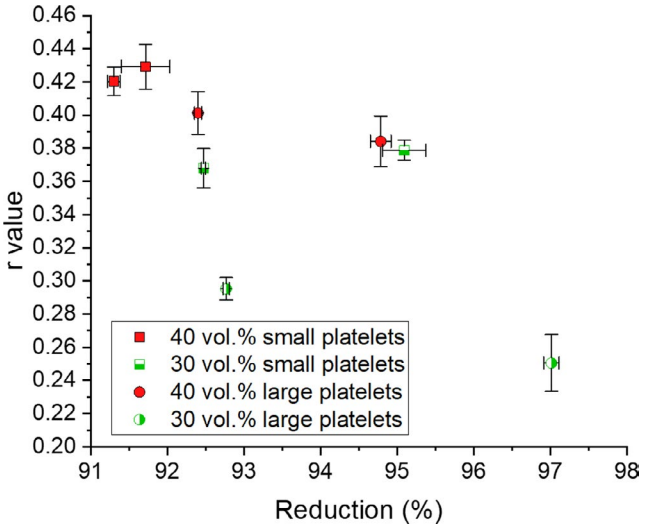

FIGURE 5 Orientation parameter (r) vs percent reduction dependence of large platelet and small blends at different solids loading. The 95% confidence interval for both the orientation parameter and percent reduction is shown for each sample having a data population of 10

when compared to large platelet blends. Due to the poor rheological properties, small platelet blends were not able to reach the target percent reductions, which leads to less biaxial extensional flow during warm pressing. As discussed earlier, the small platelet blends will have more individual particles per volume leading to an increase in particle-particle interactions, which results in inferior rheological properties and less final alignment.

It was determined that the 30 vol.% large platelet blends produced the highest average alignment. This blend was able to reach a higher percent reduction due to the rheological properties and experienced more biaxial elongational flow. Pressing this blend to a target percent reduction of 97.8% had a final alignment of $r = .251 \pm .017$, with FWHM = 11.16° ± 1.16° commonly observed in lowest alignment of $r = .429 \pm .013$, with FWHM = 25.99° ± 1.35° being produced with 40 vol.% small platelet blends at a target percent reduction of 97.8%. It is possible to develop blends with a lower solids loading (<30 vol.%), which may be able to achieve higher alignment. However, blends with lower solids loading were not investigated in this study because the resulting brown body densities would lead to samples that are too fragile for handling during hot-press die preparation. Also, it is important to note that the addition of more polymer necessitates slower binder burnout rates and longer processing times, therefore, the 30 vol.% large platelet blend pressed to 0.4 mm was chosen to produce a final pre-aligned hot-pressed sample.

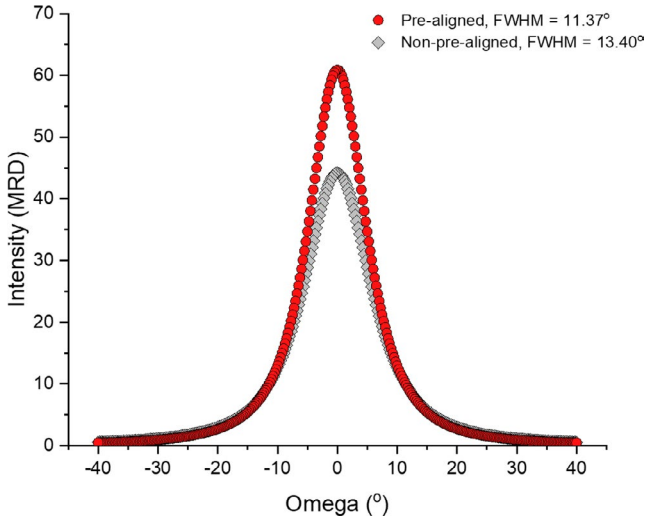

FIGURE 6 XRD rocking curves of hot-pressed non-pre-aligned and pre-aligned large platelet powders (30 vol.% large platelets blends). Pre-alignment through uniaxial warm pressing is increasing the final alignment of the transparent sample. Curves are March-Dollase fits of the data

3.4 | Analysis of hot-pressed samples

The rocking curves of hot-pressed pre-aligned and non-pre-aligned samples are shown in Figure 6. From the data, it can be seen that the pre-aligned sample has a higher peak intensity than the non-pre-aligned sample, therefore having higher alignment. The pre-aligned sample had an average alignment of $r = .254 \pm .011$ and a FWHM = 11.38° ± 0.75°, while the non-pre-aligned sample had an average alignment of $r = .283 \pm .007$ and a FWHM = 13.40° ± 0.53°. It seems that pre-aligning platelets with uniaxial warm pressing is improving the final alignment of the sintered samples. It is expected that this 14.5% decrease in the grain misalignment angle (FWHM) over non-pre-aligned samples will lead to an

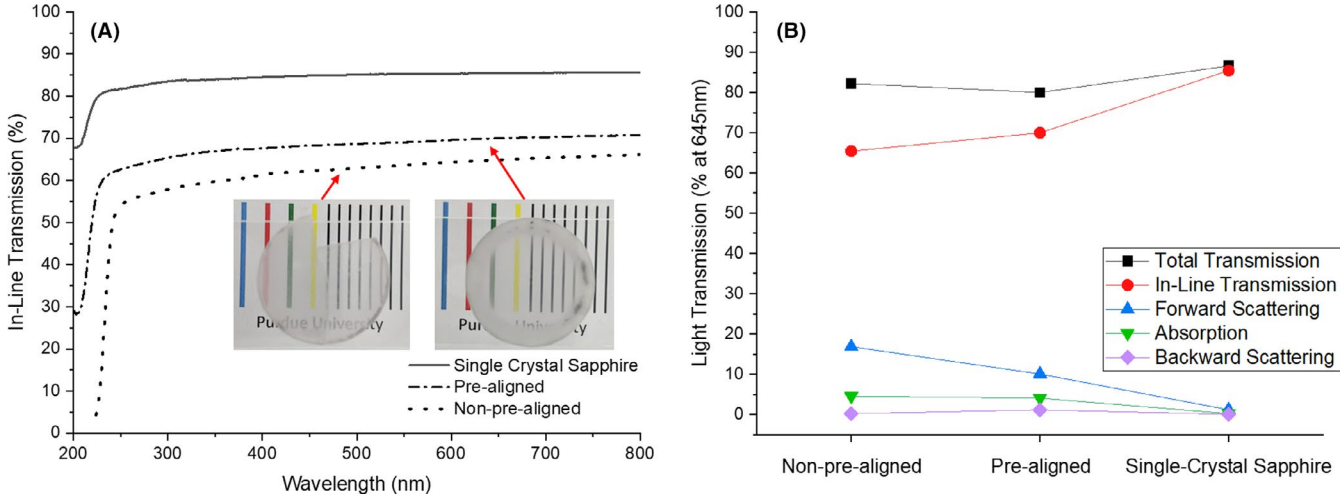

FIGURE 7 UV-Vis analysis of dense non-pre-aligned, pre-aligned, and single crystal sapphire. A, In-line transmission as a function of wavelength, normalized to $t = 0.8$ mm and (B) light transmission at 645 nm for each sample. Samples are placed 2 cm above the text. Pre-alignment of the 30 vol.% large platelet alumina blends leads to an increase in the in-line transmission when compared to non-pre-aligned alumina

improvement in the transparency.[8] In the previous study, it was found that the hot-pressing procedure is affecting the alignment of the samples.[1] However, there is no significant change in the alignment when comparing the green body sheet to the pre-aligned hot-press sample.

Figure 7A. shows the in-line transmission as a function of wavelength for the hot-pressed samples, as well as a single crystal sapphire standard. The pre-aligned sample has a higher in-line transmission compared to non-pre-aligned sample. This indicates that pre-aligning the platelets with the uniaxial warm pressing procedure is improving the optical properties. To the knowledge of the authors, this is the second highest in-line transmission reported for transparent polycrystalline alumina in the literature.[6–8,62,63] Figure 7B shows the light transmission at 645 nm for the different optical loss mechanisms. The pre-aligned sample has less forward scattering losses than the non-pre-aligned sample, which indicates lower birefringent scattering due to crystallographic alignment.[8] Both hot-pressed samples have approximately 4% absorption losses, which is indicative of trapped secondary phases.[8] As explained in previous work,[1] this absorption was minimized by performing a heat treatment at 1100°C prior to hot-pressing. The non-pre-aligned sample has effectively no backward scattering losses, while the pre-aligned sample has approximately 1% backward scattering losses. According to Apetz and Van Bruggen,8[8], backward scattering is indicative of residual porosity. In this case, it was found that the pre-aligned sample has a lower density (99.48%) than the non-pre-aligned sample (99.89%TD), which is in agreement with the backscattering data as well as a density gradient as can be seen in the outer perimeter of the pre-aligned sample in Figure 7A. The specimens with pre-aligned platelets may have a higher packing density than those that are non-pre-aligned as the oriented platelets will have a higher packing factor.[19] This lower packing density may result in a lower effective stress during hot-pressing suggesting that pre-aligned platelets may require a higher hot-pressing pressure than non-pre-aligned platelets to ultimately eliminate residual porosity and improve the final optical properties.[69] The effect of different hot-pressing pressures on pre-aligned samples will be explored in a future publication.

4 | SUMMARY AND CONCLUSIONS

Uniaxial warm pressing was used to align platelet alumina in polyethylene-based copolymers. The effects of alumina platelet solids loading and platelet diameter on viscosity, percent reduction, and final alignment were investigated. For both platelet types (large and small), decreases in the solids loading led to increases in the temperature sensitivity constant (b) and flow properties (higher shear thinning exponents (n) and lower flow consistency indices (m)). The use of small diameter platelet powders had a negative impact on the flow properties. Blends that exhibited higher temperature sensitivity constants and flow properties resulted in pressed sheets with higher percent reductions and higher final alignment. It was determined that the 30 vol.% large platelet blend was ideal for final alignment and demonstrated an average orientation value (r) and grain misalignment angle (FWHM) of 0.25 ± 0.02 and 11.16° ± 1.62°, respectively. This blend was further processed and used to produce a transparent sample that demonstrated increased optical properties when compared to non-pre-aligned samples. This sample exhibited a final orientation parameter of $r = .254 \pm .011$, a grain misalignment angle of FWHM = 11.38° ± 0.75°, and an in-line transmission of 70.0% at 645 nm. It is expected that the addition of equiaxed powder to the platelet blends will improve the rheological properties and increase the final alignment. Future analysis will investigate the use of equiaxed and platelet powder mixtures on the sinterability and alignment with the hope of increasing the final in-line transmission.

ACKNOWLEDGMENTS

This work was funded by the US Army Research Office (W911NF-17-0205). The authors thank Dr Michael Bakas from the Army Research Office. Also, Lute Lahrman and Matthew Carr for their help with processing of the samples.

ORCID

William J. Costakis https://orcid.org/0000-0002-0364-7227
Andrew Schlup https://orcid.org/0000-0001-8403-0490
Jeffrey P. Youngblood https://orcid.org/0000-0002-8720-8642
Rodney W. Trice https://orcid.org/0000-0002-8685-0289

REFERENCES

1. Schlup AP, Costakis WJ, Rheinheimer W, Trice RW, Youngblood JP. Hot-pressing platelet alumina to transparency. J Am Ceram Soc. 2019:1–15. https://doi.org/10.1111/jace.16932
2. Krell A, Klimke J, Hutzler T. Transparent compact ceramics: inherent physical issues. Opt Mater (Amst). 2009;31(8):1144–50.
3. Krell A, Klimke J, Hutzler T. Advanced spinel and sub-μm Al_2O_3 for transparent armour applications. J Eur Ceram Soc. 2009;29(2):275–81.
4. Harris DC, Johnson LF, Cambrea LR, Baldwin L, Baronowski M, Zelmon DE, et al. Refractive index of infrared-transparent polycrystalline alumina. Opt Eng. 2017;56(7):077103.
5. Peelen JGJ. Transparent hot-pressed alumina. II Transparent versus translucent alumina. Ceramurg Int. 1979;5(3):115–9.
6. Mao X, Wang S, Shimai S, Guo J. Transparent polycrystalline alumina ceramics with orientated optical axes. J Am Ceram Soc. 2008;91(10):3431–3.
7. Yi H, Mao X, Zhou G, Chen S, Zou X, Wang S, et al. Crystal plane evolution of grain oriented alumina ceramics with high transparency. Ceram Int. 2012;38(7):5557–61.
8. Apetz R, Van Bruggen MPB. Transparent alumina: a light-scattering model. J Am Ceram Soc. 2003;86(3):480–6.
9. Liu P, Yi H, Zhou G, Zhang J, Wang S. HIP and pressureless sintering of transparent alumina shaped by magnetic field assisted slip casting. Opt Mater Express. 2015;5(2):441–6.

10. Walton RL, Vaudin MD, Hofer AK, Kupp ER, Meyer RJ, Messing GL. Tailoring particle alignment and grain orientation during tape casting and templated grain growth. J Am Ceram Soc. 2019;102(5):2405–14.
11. Seabaugh MM, Messing GL, Vaudin MD. Texture development and microstructure evolution in liquid-phase-sintered α-alumina ceramics prepared by templated grain growth. J Am Ceram Soc. 2000;83(12):3109–16.
12. Seabaugh MM, Vaudin MD, Cline JP, Messing GL. Comparison of texture analysis techniques for highly oriented α-Al_2O_3. J Am Ceram Soc. 2000;83(8):2049–54.
13. Kovar D, King BH, Trice RW, Halloran JW. Fibrous monolithic ceramics. J Am Ceram Soc. 1997;80(10):2471–87.
14. Trice RW, Halloran JW. Investigation of the physical and mechanical properties of hot-pressed boron nitride/oxide ceramic composites. J Am Ceram Soc. 1999;82(9):2563–5.
15. Heuer AH, Sellers DJ, Rhodes WH. Hot-working of aluminum oxide: I, primary recrystallization and texture. J Am Ceram Soc. 1969;52(9):468–74.
16. Wu X, Chen I. Exaggerated texture and grain growth in a supperplastic SiAlON. J Am Ceram Soc. 1992;75(10):2733–41.
17. Takenaka T, Noda H, Yoneda A, Sakata K. Grain orientation effects on superconducting properties of hot-forged oxide ceramics. Ferroelectrics. 1990;102(1):329–36.
18. Watanabe H, Kimura T, Yamaguchi T. Particle orientation during tape casting in the fabrication of grain-oriented bismuth titanate. J Am Ceram Soc. 1989;72(2):289–93.
19. Reed JS. Introduction to the principles of ceramic processing. New York: Wiley, 1988.
20. Brandon D, Chen D, Chan H. Control of texture in monolithic alumina. Mater Sci Eng A. 1995;195:189–96.
21. Jabbari M, Bulatova R, Tok AIY, Bahl CRH, Mitsoulis E, Hattel JH. Ceramic tape casting: a review of current methods and trends with emphasis on rheological behaviour and flow analysis. Mater Sci Eng B. 2016;1(212):39–61.
22. Suvaci E, Seabaugh MM, Messing GL. Reaction-based processing of textured alumina by templated grain growth. J Eur Ceram Soc. 1999;19(13–14):2465–74.
23. Snel MD, van Hoolst J, de Wilde AM, Mertens M, Snijkers F, Luyten J. Influence of tape cast parameters on texture formation in alumina by templated grain growth. J Eur Ceram Soc. 2009;29(13):2757–63.
24. Pavlacka RJ, Messing GL. Processing and mechanical response of highly textured Al_2O_3. J Eur Ceram Soc. 2010;30(14): 2917–25.
25. Horn JA, Zhang SC, Selvaraj U, Messing GL, Trolier-McKinstry S. Templated grain growth of textured bismuth titanate. J Am Ceram Soc. 1999;82(4):921–6.
26. Vaudin MD, Rupich MW, Jowett M, Riley GN, Bingert JF. A method for crystallographic texture investigations using standard x-ray equipment. J Mater Res. 1998;13(10):2910–9.
27. Vaudin MD. Measurement of axisymmetric crystallographic texture. NIST. Spec Publ (NIST SP). 2009;1.
28. Raj PM, Dunn SM, Cannon WR. Measurement of particle orientation in tape cast ceramic microstructures. J Comput Assist Microsc. 1998;10(I):33–51.
29. Fu Z, Roosen A. Shrinkage of tape cast products during binder burnout. J Am Ceram Soc. 2015;98(1):20–9.
30. Park DS, Kim CW. Modification of tape casting for aligning the whiskers. J Mater Sci. 1999;34(23):5827–32.
31. Kim HJ, Krane MJM, Trumble KP, Bowman KJ. Analytical fluid flow models for tape casting. J Am Ceram Soc. 2006;89(9):2769–75.
32. Chou YT, Ko YT, Yan MF. Fluid flow model for ceramic tape casting. J Am Ceram Soc. 1987;70(10):C-280–2.
33. Luo Z, Lv Z, Jiang D, Zhang J, Chen Z, Huang Z. Aqueous tape casting of boron carbide ceramic. Ceram Int. 2013;39(2):2123–6.
34. Rahaman MN. Ceramic processing and sintering. 2nd edition. CRC Press; 2017. 1–875 pp.
35. Wonisch A, Polfer P, Kraft T, Dellert A, Heunisch A, Roosen A. A comprehensive simulation scheme for tape casting: from flow behavior to anisotropy development. J Am Ceram Soc. 2011;94(7):2053–60.
36. Knapp AM, Halloran JW. Characterization of thermoplastic blends as binders for ceramics. J Am Ceram Soc. 2006;89(10):3010–8.
37. Zhou P, Hu P, Zhang X, Han W. Laminated ZrB2-SiC ceramic with improved strength and toughness. Scr Mater. 2011;64(3):276–9.
38. Koh Y-H, Kim H-W, Kim H-E, Halloran JW. Thermal shock resistance of fibrous monolithic Si3N4/BN ceramics. J Eur Ceram Soc. 2004;24(8):2339–47.
39. Fahrenholtz WG, Hilmas GE, Chamberlain AL, Zimmermann JW. Processing and characterization of ZrB2-based ultra-high temperature monolithic and fibrous monolithic ceramics. J Mater Sci. 2004;39(19):5951–7.
40. Trice RW, Pickens EB. Ceramic Transactions Series: Innovative Processing and Synthesis of Ceramics, Glasses, and Composites VII : Proceedings of the symposium held at the 105th Annual Meeting of The American Ceramic Society, April 27-30, in Nashville, Tennessee, Ceramic Transactions, Volume 154 (1). Hoboken: Wiley-American Ceramic Society. 2012.
41. Hilmas G, Brady A, Abdali U, Zywicki G, Halloran J. Fibrous monoliths: non-brittle fracture from powder-processed ceramics. Mater Sci Eng A. 1995;195:263–8.
42. Xu X, Hilmas GE. The rheological behavior of ceramic/polymer mixtures for coextrusion processing. J Mater Sci. 2007;42(4):1381–7.
43. Koh YH, Halloran JW, Kiziltas G, Psychoudakis D, Volakis J. Thermoplastic green machining for textured dielectric substrate for broadband miniature antenna. J Am Ceram Soc. 2005;88(2):297–302.
44. Knapp AM, Halloran JW. Binder removal from ceramic-filled thermoplastic blends. J Am Ceram Soc. 2006;89(9):2776–81.
45. Kovar D, Thouless MD, Halloran JW. Crack deflection and propagation in layered silicon nitride/boron nitride ceramics. J Am Ceram Soc. 2005;81(4):1004–112.
46. Lienard SY, Kovar D, Moon RJ, Bowman KJ, Halloran JW. Texture development in Si3N4/BN fibrous monolithic ceramics. J Mater Sci. 2000;35(13):3365–71.
47. Okamoto M, Nam PH, Maiti P, Kotaka T, Nakayama T, Takada M, et al. Biaxial flow-induced alignment of silicate layers in polypropylene/clay nanocomposite foam. Nano Lett. 2001;1(9):503–5.
48. Singh AP, Rey AD. Computer simulation of dynamics and morphology of discotic mesophases in extensional flows. Liq Cryst. 1995;18(2):219–30.
49. Karnis A, Goldsmith HL, Mason SG. The kinetics of flowing dispersions. I. Concentrated suspensions of rigid particles. J Colloid Interface Sci. 1966;22(6):531–53.
50. Folgar F, Tucker CL. Orientation behavior of fibers in concentrated suspensions. J Reinf Plast Compos. 1984;3(2):98–119.
51. Jeffery GB. The motion of ellipsoidal particles immersed in a viscous fluid. Proc R Soc A Math Phys Eng Sci. 1922;102(715):161–79.

52. Trice RW, Halloran JW. Influence of microstructure and temperature on the interfacial fracture energy of silicon nitride/boron nitride fibrous monolithic ceramics. J Am Ceram Soc. 1999;82(9):2502–8.
53. Trice RW, Halloran JW. Effect of sintering aid composition on the processing of Si3N4/BN fibrous monolithic ceramics. J Am Ceram Soc. 1999;82(11):2943–7.
54. Goodrich JE, Porter RS. A rheological interpretation of torque-rheometer data. Polym Eng Sci. 1967;7(1):45–51.
55. Beeaff DR, Hilmas GE. Rheological behavior of coextruded multilayer architectures. J Mater Sci. 2002;37(6):1259–64.
56. Bousmina M, Ait-Kadi A, Faisant JB. Determination of shear rate and viscosity from batch mixer data. J Rheol (N Y N Y). 2002;43(2):415–33.
57. Blyler LL, Daane JH. An analysis of Brabender torque rheometer data. Polym Eng Sci. 1967;7(3):178–81.
58. Marquez A, Quijano J, Gaulin M. A calibration technique to evaluate the power-law parameters of polymer melts using a torque-rheometer. Polym Eng Sci. 1996;36(20):2556–63.
59. Santi CR, Hage E, Correa CA, Vlachopoulos J. Torque viscometry of molten polymers and composites. Appl Rheol. 2009;19(1):13148-1–13148-7.
60. Vaudin MD. TexturePlus | NIST [Internet]. Gaithersburg, MD: National Institute of Standards and Technology Ceramics Division; 2001 [cited 2020 Feb 4]. Available from https://www.nist.gov/publications/texture-plus
61. Chang Y, Poterala S, Yener D, Messing GL. Fabrication of highly textured fine-grained α-alumina by templated grain growth of nanoscale precursors. Suvaci E editor. J Am Ceram Soc. 2013;96(5):1390–7.
62. Pringuet A, Takahashi T, Baba S, Kamo Y, Kato Z, Uematsu K, et al. Fabrication of transparent grain-oriented polycrystalline alumina by colloidal processing. J Am Ceram Soc. 2016;99(10):3217–9.
63. Krell A, Blank P, Ma H, Hutzler T, Van Bruggen MPB, Apetz R. Transparent sintered corundum with high hardness and strength. J Am Ceram Soc. 2003;86(1):12–8.
64. Young RJ. Introduction to polymers. 2nd ed. Boca Raton, London: CRC Press, 1991.
65. Gilbert M. Relation of structure to thermal and mechanical properties. In: Brydson's plastics materials. 8th ed. Butterworth-Heinemann; 2016. p. 59–73.
66. Krieger IM, Dougherty TJ. A mechanism for non-newtonian flow in suspensions of rigid spheres. Trans Soc Rheol. 1959;3(1):137–52.
67. Malvern. Investigating the impact of particle characteristics on suspension rheology [cited 2020 Feb 4]. Available from https://www.azom.com/article.aspx?ArticleID=13727P.2017
68. Lubachevsky BD, Stillinger FH. Geometric properties of random disk packings. J Stat Phys. 1990;60(5–6):561–83.
69. Coble RL. Diffusion models for hot pressing with surface energy and pressure effects as driving forces. J Appl Phys. 1970;41(12):4798–807.

How to cite this article: Costakis WJ Jr., Schlup A, Youngblood JP, Trice RW. Aligning α-alumina platelets via uniaxial pressing of ceramic-filled polymer blends for improved sintered transparency. *J Am Ceram Soc*. 2020;00:1–13. https://doi.org/10.1111/jace.17044